F031

Application of Time Domain and Single Frequency Waveform Inversion to Real Data

D Yingst (ION Geophysical), C. Wang* (ION Geophysical), J. Park (ION Geophysical), R. Bloor (ION Geophysical), J. Leveille (ION Geophysical) & P. Farmer (ION Geophysical)

SUMMARY

A single frequency waveform inversion is advantageous over time domain inversion because of reduced cycle-skipping problems from both source signature indeterminacy and broad bandwidths. In this work we describe an implementation of both methods and begin an investigation into their comparative advantages. We describe the problem statement (in terms of cost functions) and various practical WFI strategies. Finally there is a comparison made for a real 3D marine data set.

Introduction

Waveform inversion is a method for obtaining high-fidelity velocity models for seismic imaging by minimizing some cost function of the difference between experimental and modeled wavefield data. It was introduced by Lailly, Tarantola, and Mora using a gradient-based algorithm (Lailly, 1983; Tarantola, 1984, 1987; Mora, 1986, 1988). Since then substantial research has been conducted in both the time and frequency domains (e.g. Sirgue and Pratt, 2004; Shin and Min, 2006; Vigh and Starr, 2006; Operto et al., 2007; Vigh and Starr, 2008).

Our time-domain implementation has been successfully applied to real 3D data sets. Time-domain implementations are straightforward. Their advantage is that they are relatively fast and require less memory than inverting the Helmholtz operator. Their disadvantage is significant computation time when the time or space sampling rate is small. Since the gradient is quite sensitive to time shifts, an accurate source signature delay time is necessary to match the observed and predicted data.

Various strategies such as multi-scale, layer-stripping, and offset weighting are quite useful. For instance, time domain implementations suffer from cycle-skipping when the bandwidth is too broad. This can be ameliorated using multi-scale inversion, gradually increasing the frequency bandwidth (Bunks et al., 1995). Layer-stripping inverts successively deeper layers using the presumably correct velocity model in shallower layers. This approach can be used to estimate multilayered media properties and speed up convergence. Offset-weighting localizes the data to some target region, for instance, far-offset or near-offset data. Our time domain inversion also uses a projection method to normalize the observed and modeled amplitudes.

The single-frequency approach was introduced by L. Sirgue (Sirgue, 2003). Our approach uses the time domain propagator but only one frequency for the inversion chosen to avoid cycle-skipping. It can apply the other strategies mentioned for time domain processing. It also uses a complex projection technique which allows for both amplitude and phase matching. This phase matching is novel and allows for automatic time shift computation in the source signature.

Acoustic waveform inversion in either the time or frequency domain requires low-frequency, far-offset data, as well as a relatively precise source wavelet. The problem is highly nonlinear and has many spurious local minima. Thus a good estimate of the initial velocity model is required. Also a reliable estimate of the source signature, particularly its delay time, is critical for producing accurate results. Our single-frequency inversion has the pleasant advantage that this estimation can be automated.

The paper first presents the time-domain implementation. Then it describes our single-frequency inversion. Finally it presents time and frequency domain results for a 3D marine data set.

Methods

Time-Domain Implementation

The traditional time-domain implementation is to minimize the misfit function (Tarantola, 1987):

$$\min_m J_t[m] = \|d_0 - d\|_2^2$$

where $d_0 = d_0(x_r, t, x_s)$ is the observed seismic data set and $d = d(x_r, t, x_s)$ s the predicted (i.e. computer simulated) data set for the velocity model m at source and receiver locations, x_s and x_r. The predicted data are obtained by sampling the extrapolated wavefield generated by a finite difference scheme. to the receiver locations.

We modify this cost function slightly and consider:

$$\min_m J_{pt}[m] = \|\mathbf{T}(d_0 - \rho\, d)\|_2^2,$$

where $\mathbf{T}$ is a weighting operator and ρ is an appropriate real scalar, (e.g., $\rho = \langle d, d_0 \rangle / \parallel d \parallel^2$). Note that $\mathbf{T}$ can depend on frequency, offset, and/or time. The misfit function J_{tp} is minimized iteratively by computing the gradient (Tarantola, 1984) at successive velocity models. It uses the gradient at an initial point for an initial direction estimate and updates that direction using the Polak-Ribière immplementation of the conjugate gradient (CG) method. The line search along the directions uses the BB formula (Barzilai and Borwein, 1988) for an initial steplength. It then applies the backtracking linesearch method to update the steplength.

In this case, the gradient at the k-th interation is given by

$$g_k(\mathbf{x}) = -\frac{1}{m_k^3(\mathbf{x})} \sum_{\mathbf{x}_s} \sum_t \frac{\partial^2 p}{\partial t^2}(\mathbf{x}, t; \mathbf{x}_s) r^+(\mathbf{x}, t; \mathbf{x}_s)$$

where m_k is the k-th velocity model, p is the wavefield modeled from m_k, and r^+ is the wavefield obtained by back-propagating the residual $\mathbf{T}(d_0 - \rho\, d)$.

Convergence can be accelerated using gradient pre-conditioning. Currently we only use a normalization by the amplitude of the forward-propagated wave:

Single-Frequency Implementation

To describe the single-frequency approach, let $D_0 = D_0(x_r, x_s)$ and $D = D(x_r, x_s)$ denotes the Fourier transform of d and d_0 at some fixed frequency, ω_0. (Note that D and D_0 are obtained using time propagation and not inverting the Helmholtz equation.) The standard minimization is then

$$\min_m J_f[m] = \|D_0 - D\|_2^2,$$

Again we modifie this to involve a optimal complex projection of D_0 onto D and consider

$$\min_m J_{pf}[m] = \|D_0 - \zeta\, D\|_2^2,$$

where ζ is an optimal complex scalar.

In this case the scalar has phase as well as amplitude information. We define an ω_0-dependent time shift, $T(\omega_0) = ph(\zeta)/\omega_0$. It turns out that in a certain least squares sense this is the best possible time shift for matching the ω_0*component* of the modeled and observed data. So it is used to compute the source signature time delay automatically. The gradient in this case is then similar to the time domain formulation

$$g_k(\mathbf{x}) = -\frac{\omega_0^2}{m_k^3(\mathbf{x})} \sum_{\mathbf{x}_s} Re\left(\hat{p}(\mathbf{x}, \omega_0; \mathbf{x}_s)\widehat{r^+}(\mathbf{x}, \omega_0; \mathbf{x}_s)\right),$$

except that now the residuals are obtained by back-propagating $d_0T - |\zeta|d$ where d_{0T} is d_0 shifted by $T = T(\omega_0)$. The direction calculation, pre-conditioned CG method, and linesearch are the same as in the time domain.

Results

We present an application of 3D acoustic time-domain waveform inversion to 3D marine data. Offsets ranged from 0 to 6400m. The initial velocity model for waveform inversion, 1(a), comes from a tomographic inversion.

We applied layer-stripping, muting and offset-weighting techniques in order to obtain the optimal update. The inversion proceeded in two layer-stripping steps with the inverted velocity output from one step used as the input for the next step. The first layer ranged from 1600 to 2800 m. and the second from 1600 to 4000 m. We used a single frequency band from 2 to 8.4 Hz. We also weighted far-offset data more than near-offset data using a linear weighting function.

The inverted velocity model 1(b) after 10 iterations shows a reasonable shallow update including the inferred channel system located left of center in the model. The deeper portion of the velocity model was not significantly updated because of limitations imposed by the limited maximum offset in the seismic data and the steep velocity gradient due to geology.. By finding the anomaly in lower velocity, the stack gathers 2(b) show improvement in flatness compared to the gathers using the initial velocity model 2(a).

Next, we present an application of 3D acoustic frequency-domain waveform inversion to the same data set. Like the previous inversion, comparable improvements were obtained in the shallowest portion, 1(a). The same starting model and layer stripping method as in the time domain were applied. There were 5 iterations at 5Hz and 5 iterations at 6Hz. The gathers obtained from the velocity model 1(c) are essentially identical to the ones in figure 2(b).

Conclusions

In this paper, we presented the methodolody, strategies and 3D data examples for both time-domain and single-frequency waveform inversion. A comparison shows that they are both effective and complementary methods. Both are straightforward and relatively fast (commpared to inverting the Helmholtz operator). Further, the single-frequency approach reduces cycle-skipping by limiting the bandwidth and automatically computing the source signature delay time.

Acknowledgement

The authors thank Anadarko Petroleum Corporation for permission to use the data set.

References

Barzilai, J. and Borwein, J. [1988] Two point step size gradient methods. *IMA Journal of Numerical Analysis*, **8**, 141–148.

Bunks, C., Saleck, F., Zaleski, S. and Chavent, G. [1995] Multiscale seismic waveform inversion. *Geophysics*, **60**, 457–1473.

Lailly, P. [1983] The seismic inverse problem as a sequence of before-stack migrations. In: Bednar, J. (Ed.) *Conference on Inverse Scattering: Theory and Applications*. Society for Industrial and Applied Mathematics, Philadelphia, 206–220.

Mora, P. [1986] Nonlinear 2-d elastic inversion of multi-offset seismic data. *Geophysics*, **51**, 1211–1228.

Mora, P. [1988] Elastic wavefield inversion of reflection and transmission data. *Geophysics*, **53**, 750–759.

Operto, S., Virieux, J., Amestoy, P., l'Excellent, J., Giraud, L. and Ali, H. [2007] 3d finite-difference frequency-domain modeling of viscoacoustic wave propagation using a massively parallel direct solver: A feasibility study. *Geophysics*, **72**(5), SM195–SM211.

Shin, C. and Min, D. [2006] Waveform inversion using a logarithmic wavefield. *Geophysics*, **71**(3), R31–R42.

Sirgue, L. [2003] *Inversion de la forme d'onde dans le domaine fréquentiel de données sismiques grands offsets*. Ph.D. thesis, l'Ecole Normale Supéreure de Paris, Queen's University.

Sirgue, L. and Pratt, R. [2004] Efficient waveform inversion and imaging: A strategy for selecting temporal frequencies. *Geophysics*, **69**, 231–248.

Tarantola, A. [1984] Inversion of seismic reflection data in the acoustic approximation. *Geophysics*, **49**, 1259–1266.

Tarantola, A. [1987] *Inverse Problem Theory*. Elsevier.

Vigh, D. and Starr, E. [2006] Shot profile versus plane wave reverse time migration. *76th Annual International Meeting, SEG*, 2358–2361, expanded Abstract.

Vigh, D. and Starr, E. [2008] 3d prestack plane-wave, full-waveform inversion. *Geophysics*, **73**, VE135–VE144.

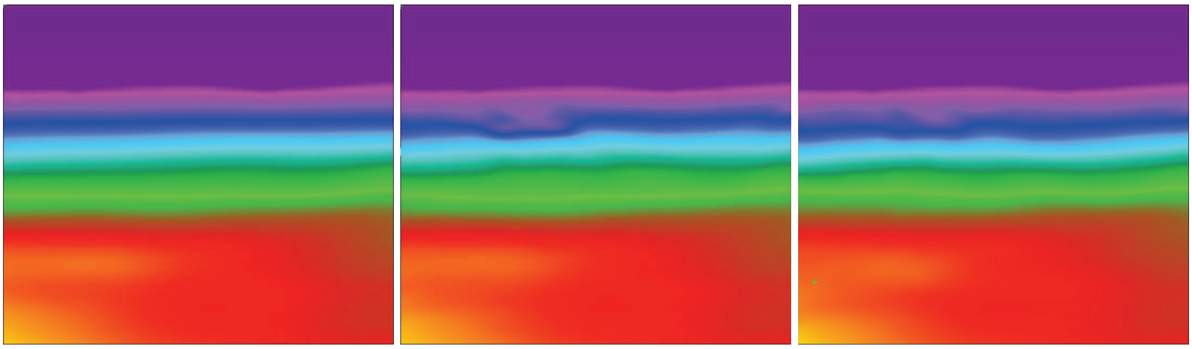

(a) Initial velocity model (b) TD inverted model after 10 iterations (c) SF inverted model after 10 iterations

Figure 1 *3D velocity model*

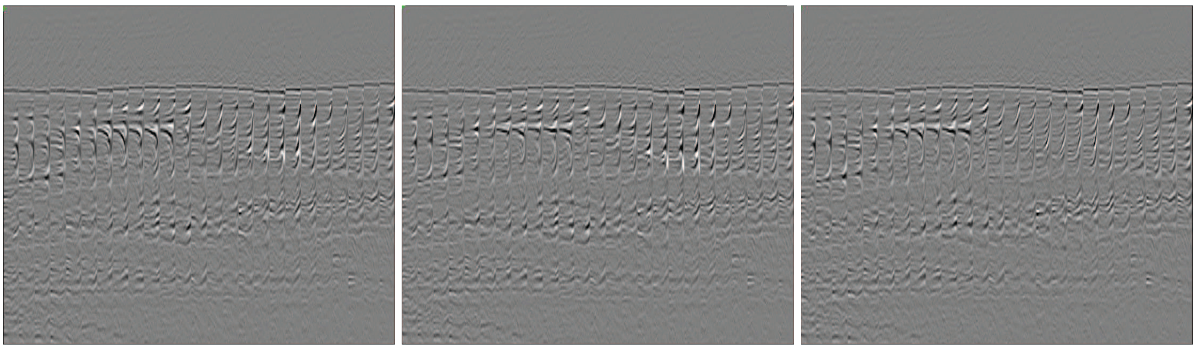

(a) Initial model gather (b) Updated time domain gather (c) Updated single frequency gather

Figure 2 *3D gathers*